Journal of Cluster Science, Vol. 18, No. 1, March 2007 (© 2006)
DOI: 10.1007/s10876-006-0074-9

The Physical and Electronic Structure of M_2 Quadruply Bonded Complexes: A Density Functional Theory Study

Malcolm H. Chisholm,[1] Jason S. D'Acchioli,[2,3] and Christopher M. Hadad[1]

Received July 28, 2006; published online September 17, 2006

The electronic structures and the physical properties (vertical excitation energies, vibrational stretching frequencies, and bond lengths) of a variety of M–M quadruply bonded (M = Mo, W) complexes are investigated using density functional theory (DFT). By utilizing a variety of pure and hybrid exchange-correlation (XC) functionals and a number basis sets, we are able to recommend a theoretical methodology for most efficiently probing the electronic structures of homoleptic $M_2(O_2CR)_4$ and bridged $M_2(O_2C\text{-}X\text{-}CO_2)M_2$ (R = organic group, typically H; X = conjugated organic group) complexes.

KEY WORDS: Density functional theory; metal–metal quadruple bonds; time-dependent density functional theory; paddlewheel complexes.

INTRODUCTION

Electronic structure calculations on metal–metal quadruply bonded (M_2) complexes of the form $M_2(O_2CH)_4$ have been a source of interest for over 30 years [1]. The earliest calculation on a M_2 paddlewheel complex was a Xα-SW computational study of $Mo_2(O_2CH)_4$ by Norman and coworkers (Fig. 1) [2–4]. The results of the calculation established the qualitative assumption that Cotton and coworkers had made several years prior [5], namely that the frontier M_2 molecular orbitals (MOs) consisted of σ, π, and

[1]Department of Chemistry, The Ohio State University, 100 W. 18th Avenue, Columbus, OH 43210-1185, USA.
[2]Department of Chemistry, University of Wisconsin-Stevens Point, 2001 Fourth Avenue, Stevens Point, WI 54481-1911, USA.
[3]To whom correspondence should be addressed. E-mail: jdacchio@uwsp.edu

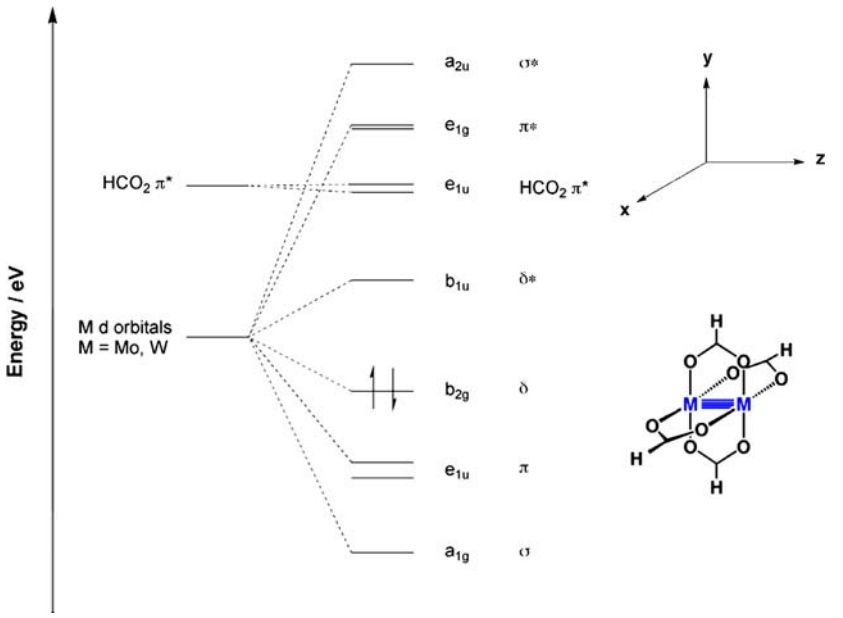

Fig. 1. Qualitative MO diagram for $Mo_2(O_2CH)_4$. Only the HOMO is showed as filled for clarity.

δ combinations of the metal d orbitals with the bonding combinations being totally filled. Beyond a correct assessment of bonding, however, Xα-SW was remarkably poor in approximating vertical excitation energies in $Mo_2(O_2CH)_4$ beyond a qualitative ordering of energies.

As computational methodologies and facilities matured, M_2 carboxylate complexes continued to attract the attention of computational chemists [1–3, 6–10]. One experimental observable which received tremendous attention was computation of the energy of the M_2 $\delta \rightarrow \delta^*$ transition. The transition can be difficult to observe experimentally since it is often masked by the much more intense M_2 $\delta \rightarrow CO_2$ π^* transition [11]. It is, nonetheless, observable, and finding a computational method to evaluate it accurately would be invaluable. This is easier said than done, however.

The central problem surrounding calculations of the M_2 $\delta \rightarrow \delta^*$ transition is electron correlation. Many researchers have treated this problem in great detail, and a full treatment will not be given here [12–15]. It is sufficient to say that, using traditional *ab initio* methods, there is no way to adequately describe the electronic configuration associated with the M_2 $\delta \rightarrow \delta^*$ transition. If one treats the situation as a

two electrons in two orbitals problem, it can be shown that four configurations composed of different combinations of Slater determinants are needed to adequately describe the $\delta \rightarrow \delta^*$ electronic state. As such, the problem cannot be treated effectively with single-determinantal *ab initio* methods. Hall stated this difficulty in an eloquent manner in the title of his 1987 *Polyhedron* article, ''Problems in the Theoretical Description of Metal–Metal Multiple Bonds or How I Learned to Hate the Electron Correlation Problem'' [16].

One of the earliest implementations of density functional theory (DFT), Xα-SW [17, 18], was an improvement over *ab initio* methods. The main benefit of Xα-SW was the natural inclusion of *some* electron correlation, an artifact of electrons having opposite spin. The computational results were reasonable, and made sense in terms of a qualitative bonding analysis. Calculated analogues of experimental observables such as vertical excitation energies however, were still markedly poor. Indeed, the calculated value of the $\delta \rightarrow \delta^*$ transition in $Mo_2(O_2CH)_4$ was $9.2 \times 10^3\ cm^{-1}$, while the experimental value was $18.8 \times 10^3\ cm^{-1}$!

As DFT methods improved, so did the quality of their results. In some of the first modern DFT studies on M_2 quadruply bonded paddlewheel complexes (M = Mo, Nb, Tc, Re) [19, 20], Cotton and coworkers established an effective prescription for evaluating electronic structures. Their choice of the hybrid B3LYP exchange-correlation (XC) functional, coupled with a double-zeta (DZ) quality basis set (D95) [21] on ligand atoms and the LanL2DZ basis set [22–24] and effective core potential (ECP) on the transition metal, has been a cornerstone of their computational investigations [19, 20, 25–28]. In retrospect, their choices made good sense. A DZ basis set is sufficiently flexible for ligand atoms, and the use of the LanL2DZ basis set and ECP would account for relativistic effects; the B3LYP [29–31] XC functional had been heavily utilized—with good results—in the literature [32]. The results obtained by Cotton and coworkers compared favorably to their experimental observables, including bond lengths from X-ray crystal structures, vibrational stretching frequencies, and vertical excitation wavelengths [19, 20, 25–28].

As work in this laboratory has progressed in a similar vein to Cotton *et al.* (*vide infra*), computational conventions have been adopted. A glance through publications from the past 5 years shows that we, too, utilize the B3LYP XC functional, yet we favor the 6-31G* Pople basis set [33] on ligand atoms, and the Stuttgart–Dresden (SDD) [34] basis set and ECP on transition metal centers. Given that Cotton *et al.* and this laboratory use slightly different methodologies on comparable systems, coupled with the seemingly endless number of density functionals and basis sets available, a question is raised—what is the ''best'' methodology? There is sometimes a

temptation to treat computational chemistry as a "black-box", without ever truly understanding its mechanics. With this as an impetus, we have performed electronic structure calculations on a variety of M_2 quadruply bonded complexes, utilizing a variety of basis sets and XC functionals. With the results herein, we can make an informed decision about which level of theory is better suited for our particular systems.

COMPUTATIONAL DETAILS

All calculations were performed using density functional theory as implemented in the Gaussian03 suite of programs (revisions b.04 and c.02) [35]. Model complexes of the form D_{4h}-$[M_2(O_2CR)_4]^{0/+\bullet}$, D_{2h}-$[(RCO_2)_3M_2]_2(\mu\text{-}O_2CCO_2)]^{0/+\bullet}$, and D_{2h}-$[(RCO_2)_3M_2]_2(\mu\text{-}O_2CC_6F_6CO_2)]^{0/+\bullet}$ (R = H, M = Mo, W) (Fig. 2) were geometry-optimized in their respective point groups. Experimental data for each complex were taken from solution studies of the R = ^{t}Bu complexes. It should be noted that only the planar form of D_{2h}-$[(HCO_2)_3M_2]_2(\mu\text{-}O_2CC_6F_6CO_2)]^{0/+\bullet}$ was considered in this study, since there is both experimental and spectroscopic evidence that this is the preferred ground state structure [36].

In order to ascertain which ECP would work best for Mo and W, we used $M_2(O_2CH)_4{}^{0/+\bullet}$ as test cases. The Mo and W basis sets and ECPs chosen were SDD [34], and LanL2DZ [22–24], while the ligand atom basis set was held constant at 6-31G*. Seven of the more "popular" XC functionals—B3LYP [29–31], B3P86 [29, 31, 37], B3PW91 [29, 31, 38–45], PBE1PBE [43, 44], BLYP [30, 31], BPW91 [31, 38–42, 45], and PW91PW91 [38–42, 45]—were then utilized in the calculation of bond lengths, vibrational frequencies, and excitation energies via time-dependent density functional theory (TD-DFT) [46–48] as implemented in the Gaussian suite of programs. All calculated observables were compared to experimental values [49], and the most appropriate metal basis sets and XC functionals were chosen.

The efficacy of a variety of basis sets was analyzed for the ligand atoms, namely the 3-21G, 6-31G*, and 6-31 + G* Pople basis sets [33], as well as Dunning's aug-cc-pVDZ basis set. From the results of the $M_2(O_2CH)_4{}^{0/+\bullet}$ calculations, the most appropriate basis sets and XC functionals were used for geometry optimizations, vibrational frequency analyses, and TD-DFT calculations on the model complexes D_{2h}-$[(HCO_2)_3M_2]_2(\mu\text{-}O_2CCO_2)]^{0/+\bullet}$ and D_{2h}-$[(HCO_2)_3M_2]_2(\mu\text{-}O_2CC_6F_6CO_2)]^{0/+\bullet}$, and the results compared to experimental observables. It should be noted that all model complexes were found to be local minima on their respective potential energy surfaces, regardless of the level of theory used.

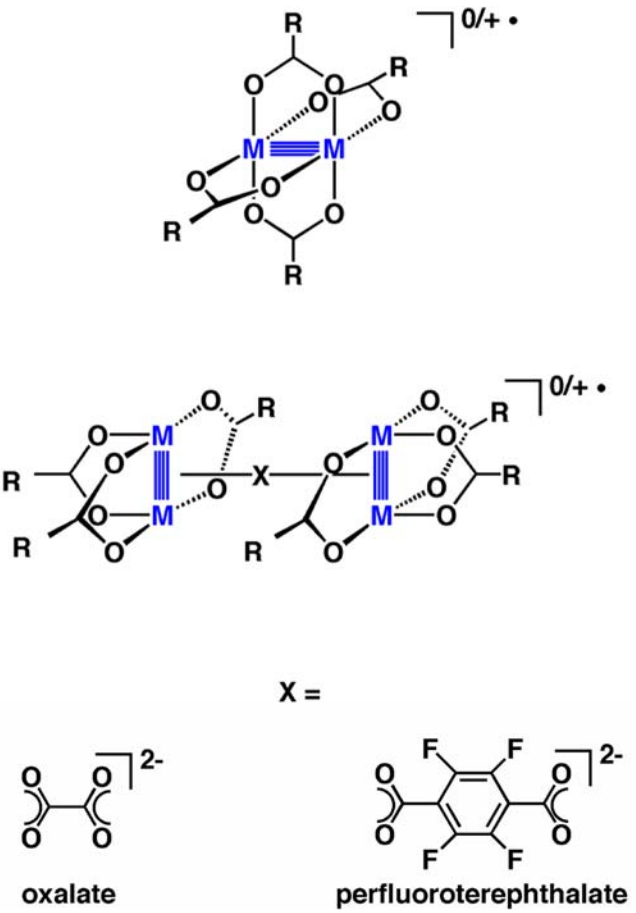

Fig. 2. Model complexes considered in this study.

RESULTS AND DISCUSSION

Selection of ECP: $M_2(O_2CH)_4$ Model Complexes

The process of choosing a basis set for a transition metal is not a trivial one. Transition metals have many electrons, making their involvement in electronic structure calculations problematic. As it is relevant to current work in this laboratory, we will consider only the second and third row transition metals, Mo and W. Mo has 42 electrons, while W has 74 electrons. If all electrons in both Mo and W were considered in a DFT calculation—a so-called "all electron" calculation—the amount of time

spent evaluating correlation and exchange would be prohibitively large. Even in the most optimistic scenario, the time it takes to optimize the geometry of a system with N electrons scales as N^3 [50]. Calculations on M_2 systems would appear even more difficult; the largest system in this study, $[(HCO_2)_3W_2]_2(\mu\text{-}O_2CC_6F_6CO_2)]$, contains four tungsten centers and 42 main group elements, for a total of 568 electrons! The matter can be greatly simplified through the use of an ECP.

The LanL2DZ ECP of Hay and Wadt [22–24] and the SDD energy-consistent ECP of the Stuttgart group [34] have been used by Cotton and coworkers and Chisholm and coworkers, respectively; both will be considered herein. Both the LanL2DZ and SDD ECPs treat the $ns^2np^6nd^q(n + 1)s^2$ electrons (14 electrons for Mo and W, $n = 4$ or 5) as valence, with all other electrons being considered as core.[1] It has been shown that including the $ns^2np^6nd^q(n + 1)s^2$ electrons as valence often gives better descriptions of transition metal bonding, including cases where multiple bonding between metal atoms occurs [23].

Another, and perhaps more important, reason for using ECPs is their inherent inclusion of relativistic effects. In an excellent paper on the subject, Katsolyannis described how, as a consequence of Einstein's special theory of relativity, electrons would experience a relativistic mass increase of the form

$$m = \frac{m_0}{\sqrt{1 - (v_{rad}/c)^2}} \tag{1}$$

where m_0 is the mass of a particle (in our case, an electron); v is the velocity of the electron; c is the speed of light; and m is the mass of the electron after acceleration. It is obvious that as v approaches the speed of light the mass of the electron would become infinite [51]. This effect is dramatic. There is a contraction, primarily pertaining to the core s and p electrons, leading to increased shielding and a net expansion of the d and f orbitals. For example, Mo experiences a contraction of 4.8%, while W contracts nearly 16%. The relativistic phenomenon has significant implications with respect to bonding.

There are two fundamental differences between the LanL2DZ and SDD ECPs. The first difference is that the SDD ECPs have been adjusted to the valence energies of a number of atomic reference states, thus introducing a link to experimental observables [34]. The LanL2DZ ECP, however, is generated by comparison to results from all-electron *ab initio* calculations. The parameters used for comparison in the LanL2DZ case, e.g. molecular

[1]The q in $ns^2np^6nd^q(n + 1)s^2$ refers to the number of d electrons for a particular transition metal.

orbital shapes and energies, are not direct experimental observables. The second difference between the two ECPs is the way valence electrons are treated. The general contraction scheme of the LanL2DZ ECP is (8s6p4d)/[3s3p2d], while that for the SDD ECP is (8s7p6d)/[6s5p3d].[2] While the SDD basis set might appear to be more flexible and to have a better description of its core electrons, this does not necessarily mean it is the "better" basis set (*vide infra*). Justification of the more appropriate ECP can only be made after analyzing the results from electronic structure calculations on a test set of model complexes. Utilizing the D_{4h}-$[M_2(O_2CH)_4]^0$ model complexes (M = Mo or W) (Fig. 1), bond lengths, vibrational frequencies, and vertical excitation energies were calculated with the 6-31G* Pople basis set on O, C, and H, and with the B3LYP, B3P86, B3PW91, PBE1PBE, BLYP, BPW91, and PW91PW91 XC functionals. Absolute errors (AEs) and mean absolute errors (MAEs) for all data are compiled in Tables I–III.

As shown in Table I the LanL2DZ ECP performs 0.003–0.006 Å better than the SDD ECP for M-M and M-O bond lengths. The one exception is where the B3LYP XC functional is utilized; in that case, the SDD ECP performs 0.053 Å better than the LanL2DZ ECP. The trend, however, is reversed in the case of M–M stretching frequencies. Table II illustrates that, on average, the SDD ECP performs 2.65–21.61 cm^{-1} better than the LanL2DZ ECP. Again, the B3LYP XC functional illustrates the most interesting result, as the SDD ECP performs 21.61 cm^{-1} better than the LanL2DZ ECP. While the $\delta \rightarrow \delta^*$ electronic transition was calculated, there is, unfortunately, no firm experimental evidence for the $W_2(O_2CH)_4$ $\delta \rightarrow \delta^*$ transition. As such, MAEs cannot be utilized. From an inspection of Table III, however, it is quite evident that the SDD ECP out-performs the LanL2DZ ECP, being 7.14–11.3 nm closer to the experimental values.

Selection of XC Functionals: $M_2(O_2CH)_4$ Model Complexes

With the selection of the SDD ECP as the Mo and W basis set of choice, our attention turned to which XC functionals we should investigate. While there are many functionals for treating transition metal species [52], we have narrowed our scope for the existing problem (*vide infra*). Utilizing the same D_{4h}-$[M_2(O_2CH)_4]^0$ (M = Mo, W) data set, judicious decisions were made about which XC functionals should be studied further. Since the majority of recent M_2 calculations have utilized the hybrid B3LYP XC functional, we chose to keep it throughout the rest of the study [19, 20, 25–27, 36, 49, 53–59]. Also, since work from this laboratory has utilized the

[2]The ()/[] notation is referred to as a general contraction scheme. The values in () are PGTOs, which are reduced to the CGTOs in [].

Table I. AEs and MAEs of M–M and M–O (M = Mo, W) bond lengths (Å) in the model complex D_{4h}-$M_2(O_2CH)_4$ using the SDD and LanL2DZ ECPs across arange of XC functionals

ECP		B3LYP AE	B3P86 AE	B3PW91 AE	PBE1PBE AE	BLYP AE	BPW91 AE	PW91PW91 AE
SDD	Mo_2	0.032	0.020	0.021	0.012	0.070	0.053	0.054
	W_2	0.024	0.012	0.013	0.005	0.057	0.040	0.041
LanL2DZ	Mo_2	0.036	0.025	0.025	0.019	0.072	0.056	0.058
	W_2	0.222	0.001	0.002	0.004	0.041	0.026	0.028
SDD	Mo–O	0.011	0.008	0.003	0.007	0.023	0.005	0.001
	W–O	0.031	0.014	0.019	0.015	0.043	0.026	0.021
LanL2DZ	Mo–O	0.014	0.006	0.001	0.003	0.028	0.011	0.004
	W–O	0.021	0.003	0.003	0.002	0.027	0.011	0.006
MAE SDD		0.024	0.013	0.014	0.010	0.048	0.031	0.029
MAE LanL2DZ		0.073	0.009	0.008	0.007	0.042	0.026	0.024

The 6-31G* basis set was used on C, H, and O.

Table II. AEs and MAEs of M–M (M = Mo, W) bond stretching vibrational frequencies (cm^{-1}) for the model complex D_{4h}-$M_2(O_2CH)_4$ using the SDD and LanL2DZ ECPs across a range of XC functionals

ECP		B3LYP AE	B3P86 AE	B3PW91 AE	PBE1PBE AE	BLYP AE	BPW91 AE	PW91PW91 AE
MWB	Mo_2	60.93	72.13	70.55	78.01	29.27	42.65	42.90
	W_2	20.48	29.22	28.49	33.89	2.23	8.68	7.91
LanL2DZ	Mo_2	83.24	77.44	76.33	83.24	34.78	48.28	48.01
	W_2	41.38	29.22	36.31	41.38	6.90	17.47	16.65
MAE SDD		40.70	50.68	49.52	55.95	15.75	25.66	25.41
MAE LanL2DZ		62.31	53.33	56.32	62.31	20.84	32.88	32.33

The 6-31G* basis set was used on C, H, and O.

Table III. AEs and MAEs of $\delta \rightarrow \delta^*$ vertical transition energies (nm) for the model complex D_{4h}-$M_2(O_2CH)_4$(M = Mo, W) using the SDD and LanL2DZ ECPs across a range of XC functionals

ECP		B3LYP AE	B3P86 AE	B3PW91 AE	PBE1PBE AE	BLYP AE	BPW91 AE	PW91PW91 AE
SDD	Mo_2	72.13	45.45	48.76	57.11	32.04	9.19	6.42
	W_2				NA			
LanL2DZ	Mo_2	83.43	55.03	58.56	67.94	39.64	16.33	13.62
	W_2				NA			

The 6-31G* basis set was used on C, H, and O.

PW91PW91 XC functional (albeit as implemented in the Amsterdam Density Functional (ADF) suite of programs) [60], we decided to further investigate its behavior.

To keep the study consistent, we decided to choose both another hybrid and pure XC functional. This posed the rather difficult task of choosing which set of criteria were more important to model, particularly if some methods performed better for certain parameters, e.g. vibrational frequencies, than others, e.g. vertical excitation energies. The choice of the second hybrid functional was a fairly easy one to make. Compared to the PBE1PBE XC functional, B3P86 had the second lowest bond length MAE, and the lowest MAE for the $Mo_2(O_2CH)_4$ $\delta \rightarrow \delta^*$ transition. With respect to vibrational frequencies, even though B3PW91 had the second lowest (relative to B3LYP) MAE of 49.52 cm^{-1}, B3P86 was very close with a MAE of 50.68 cm^{-1}. Taking the aforementioned factors into consideration, B3P86 was chosen as the second hybrid XC functional.

Choosing the final XC functional was really a choice between the pure XC functionals BLYP and BPW91. BPW91 gave a bond length MAE 0.017 Å lower than that for BLYP, while BLYP gave a vibrational frequency MAE which was 9.91 cm^{-1} lower than BPW91. The decision ultimately came down to the magnitude of the MAEs for the $Mo_2(O_2CH)_4$ $\delta \rightarrow \delta^*$ excitation energy—BPW91 had an MAE which was 22.85 nm lower than BLYP's. Given a choice between a better vibrational frequency or excitation energy, we chose excitation energy, as UV–visible spectroscopy is an integral part of our research.

Selection of Basis Sets on Non-metal Atoms $M_2(O_2CH)_4^{0/+\bullet}$ Model Complexes

With the choice of both metal basis set and XC functionals in hand, we then turned our attention to the choice of basis set on non-metal atoms, i.e. C, H, O, and F, in our model complexes of interest. There are many choices with respect to basis set selection, and one needs to carefully weigh performance with computational expense. We have chosen to test, in order of increasing size, the 3-21G, 6-31G*, 6-31+G*, and aug-cc-pVDZ Gaussian-type basis sets. We again use the $M_2(O_2CH)_4$ test set (M = Mo, W); however, we expand this set to include the radical cations $M_2(O_2CH)_4^{+\bullet}$, as many such species are readily isolated in this laboratory [49, 58].

Tables IV–XI provide M–M and M–O bond lengths, M–M vibrational stretching frequencies, and $\delta \rightarrow \delta^*$ vertical transition energies for $M_2(O_2CH)_4^{0/+\bullet}$ model complexes (M = Mo, W). An inspection of the data reveals two important trends. The first is the 3-21G basis set tends to offer the highest AE for any property. A very notable exception to this argument

Table IV. AEs of Mo–Mo bond lengths (Å) across a range of XC functionals in the model complex D_{4h}-$Mo_2(O_2CH)_4^{0/+\bullet}$ using the SDD ECP on Mo while varying the basis set on C, H, and O

Basis set	B3LYP AE	B3P86 AE	BPW91 AE	PW91PW91 AE
3-21G	0.0534	0.0420	0.0732	0.0745
6-31G*	0.0317	0.0200	0.0533	0.0543
6-31 + G*	0.0327	0.0204	0.0540	0.0557
aug-cc-pVDZ	0.0307	0.0187	0.0522	0.0543
3-21G$\|^{+\bullet}$	0.0364	0.0228	0.0526	0.0540
6-31G*$\|^{+\bullet}$	0.0144	0.0007	0.0325	0.0334
6-31 + G*$\|^{+\bullet}$	0.0147	0.0003	0.0337	0.0337
aug-cc-pVDZ $\|^{+\bullet}$	0.0101	0.0043	0.0292	0.0292

Table V. AEs of Mo-O bond lengths (Å) across arange of XC functionals in the model complex D_{4h}-$Mo_2(O_2CH)_4^{0/4\cdot}$ using the SDD ECP on Mo while varying the basis set on C, H, and O

Basis set	B3LYP AE	B3P86 AE	BPW91 AE	PW91PW91 AE
3-21G	0.0177	0.0358	0.0216	0.0273
6-31G*	0.0106	0.0085	0.0054	0.0007
6-31 + G*	0.0125	0.0076	0.0069	0.0010
aug-cc-pVDZ	0.0064	0.0149	0.0007	0.0059
3-21G $\|^{+\bullet}$	0.0059	0.0219	0.0038	0.0092
6-31G*$\|^{+\bullet}$	0.0116	0.0047	0.0134	0.0085
6-31 + G*$\|^{+\bullet}$	0.0122	0.0049	0.0137	0.0090
aug-cc-pVDZ I $^{+\bullet}$	0.0073	0.0101	0.0085	0.0038

appears in Table VII. The $M_2(O_2CH)_4^{0/+\bullet}$ $\delta \rightarrow \delta^*$ transition values at both the B3LYP and B3P86 levels of theory are predicted to have much lower AEs than the larger basis sets in the series. The trend does not hold true, however, when the BPW91 and PW91PW91 XC functionals are used; the results are worse. The second trend is that utilizing a larger basis set, i.e. the 6-31 + G* or aug-cc-pVDZ, does not necessarily yield better results.

The 3-21G basis set is the smallest used in this study. It does not, in general, have the mathematical flexibility necessary to describe bonding effectively, and is known to give less accurate results [33]. If we compare the contraction schemes for the 3-21G basis set, (6s3p/3s)/[3s2p/2s],[3] with the

[3]The (6s3p/3s)/[3s2p/2s] notation again refers to a contraction scheme (*vide supra*). The / mark in each set of parentheses separates a description of non-hydrogen atoms (to the left of the /) from hydrogen atoms (to the right of the /).

Table VI. AEs of Mo-Mo stretching vibrational frequencies (cm^{-1}) across a range of XC functionals in the model complex D_{4h}-$Mo_2(O_2CH)_4^{0/+\bullet}$ using the SDD ECP on Mo while varying the basis set on C, H, and O

Basis set	B3LYP AE	B3P86 AE	BPW91 AE	PW91PW91 AE
3-21G	60.69	73.18	46.36	48.31
6-31G*	60.93	72.13	42.65	42.90
6-31 + G*	58.30	72.13	40.47	40.23
aug-cc-pVDZ	60.46	72.28	42.30	41.88
3-21G $\|^{+\bullet}$	49.85	61.75	34.92	37.11
6-31G*$\|^{+\bullet}$	44.87	55.77	28.83	30.50
6-31 + G*$\|^{+\bullet}$	42.90	54.57	27.35	28.61
aug-cc-pVDZ $\|^{+\bullet}$	66.21	58.41	30.53	31.87

contraction scheme for the 6-31G* basis set, (10s4p/4s)/[3s2p/2s], it is easy to see the latter is more flexible, since it contains more PGTOs [50]. Since the 3-21G basis set provides larger AEs than the other basis sets, we will no longer consider it. Considering the remaining basis sets, i.e. 6-31G*, 6-31 + G*, and aug-cc-pVDZ, which is more efficient and cost-effective? This is a fairly straightforward question to answer. Examination of the AEs in Tables VII–XI shows the 6-31G*, 6-31 + G*, and aug-cc-pVDZ basis sets to be fairly consistent. In many cases, especially with M–M stretching vibrational frequencies (Tables VI and X), the aug-cc-pVDZ basis set performs *less* accurately than either 6-31G* or 6-31 + G*. Perhaps the strongest argument against using the aug-cc-pVDZ basis set, though, is cost in terms of computational resources. Table XII shows the CPU time required for the simplest model systems in this study, $M_2(O_2CH)_4$ (M = Mo, W). The cost of running a calculation with the aug-cc-pVDZ basis set is considerably longer—by *days* for vibrational frequency analyses!—than the 6-31G* basis set. More importantly, the quality of results using the aug-cc-pVDZ basis set are not any better (or, in some cases, any worse) than results using the more economical 6-31G* basis set. A similar argument can be made for not using the 6-31 + G* basis set. While not as large as the aug-cc-pVDZ basis set, it is still costly in terms of computational resources. Use of the 6-31 + G* basis set also presented convergence problems for $W_2(O_2CH)_4^{0/+\bullet}$ at the B3LYP and PW91PW91 levels of theory. Considering the factors of cost and efficiency, the 6-31G* basis set is deemed an appropriate choice.

Before continuing, it is important to make a note on the use of AEs. While AEs are appropriate for gauging a method, it does not indicate whether the method either over- or under-estimates an experimental

Table VII. AEs of $\delta \rightarrow \delta^*$ vertical transition energies (nm) across a range of XC functionals in the model complex D_{4h}-$Mo_2(O_2CH)_4^{0/+\bullet}$ using the SDD ECP on Mo while varying the basis set on C, H, and O

Basis set	B3LYP AE	B3P86 AE	BPW91 AE	PW91PW91 AE
3-21G	38	13	14	17
6-31G*	72	45	9	6
6-31 + G*	77	49	12	9
aug-cc-pVDZ	74	46	10	9
3-21G *$\vert^{+\bullet}$	45	22	174	184
6-31G*$\vert^{+\bullet}$	131	53	132	140
6-31 + G*$\vert^{+\bullet}$	140	59	128	136
aug-cc-pVDZ $\vert^{+\bullet}$	126	45	133	141

Table VIII. AEs of W–W bond lengths (Å) across a range of XC functionals in the model complex D_{4h}-$W_2(O_2CH)_4^{0/+\bullet}$ using the SDD ECP on W while varying the basis set on C, H, and O

Basis set	B3LYP AE	B3P86 AE	BPW91 AE	PW91PW91 AE
3-21G	0.0445	0.0316	0.0575	0.0586
6-31G*	0.0245	0.0116	0.0397	0.0409
6-31 + G*	NA	0.0121	0.0404	NA
aug-cc-pVDZ	0.0244	0.0114	0.0391	0.0406
3-21G *$\vert^{+\bullet}$	0.0423	0.0284	0.0531	0.0542
6-31G*$\vert^{+\bullet}$	0.0227	0.0089	0.0352	0.0362
6-31 + G*$\vert^{+\bullet}$	0.0228	0.0083	0.0347	0.0364
aug-cc-pVDZ $\vert^{+\bullet}$	0.0191	0.0044	0.0314	0.0327

Table IX. AEs of W–O bond lengths (Å) across a range of XC functionals in the model complex D_{4h}-$W_2(O_2CH)_4^{0/+\bullet}$ using the SDD ECP on W while varying the basis set on C, H, and O

Basis set	B3LYP AE	B3P86 AE	BPW91 AE	PW91PW91 AE
3-21G	0.0057	0.0104	0.0026	0.0021
6-31G*	0.0307	0.0136	0.0262	0.0209
6-31 + G*	NA	0.0135	0.0268	NA
aug-cc-pVDZ	0.0306	0.0072	0.0212	0.0161
3-21G $\vert^{+\bullet}$	0.0172	0.0024	0.0179	0.0136
6-31G* $\vert^{+\bullet}$	0.0325	0.0168	0.0331	0.0287
6-31 + G* $\vert^{+\bullet}$	0.0326	0.0160	0.0330	0.0287
aug-cc-pVDZ $\vert^{+\bullet}$	0.0285	0.0118	0.0285	0.0243

Table X. AEs of W–W stretching vibrational frequencies (cm^{-1}) across a range of XC functionals in the model complex D_{4h}-$W_2(O_2CH)_4^{0/+\bullet}$ using the SDD ECP on W while varying the basis set on C, H, and O

Basis set	B3LYP AE	B3P86 AE	BPW91 AE	PW91PW91 AE
3-21G	13.66	22.51	3.27	2.47
6-31G*	20.48	29.22	8.68	7.91
6-31 + G*	NA	28.54	7.97	NA
aug-cc-pVDZ	20.65	29.50	9.20	8.24
3-21G | $^{+\bullet}$	NA	NA	NA	NA
6-31G* | $^{+\bullet}$	NA	NA	NA	NA
6-31 + G* | $^{+\bullet}$	NA	NA	NA	NA
aug-cc-pVDZ | $^{+\bullet}$	NA	NA	NA	NA

Table XI. AEs of $\delta \rightarrow \delta^*$ vertical transition energies (nm) across a range of XC functionals in the model complex D_{4h}-$W_2(O_2CH)_4^{0/+\bullet}$ using the SDD ECP on W while varying the basis set on C, H, and O

Basis set	B3LYP AE	B3P86 AE	BPW91 AE	PW91PW91 AE
3-21G	NA	NA	NA	NA
6-31G*	NA	NA	NA	NA
6-31 + G*	NA	NA	NA	NA
aug-cc-pVDZ	NA	NA	NA	NA
3-21G | $^{+\bullet}$	152	301	262	267
6-31G* | $^{+\bullet}$	78	117	216	222
6-31 + G* | $^{+\bullet}$	71	112	211	217
aug-cc-pVDZ | $^{+\bullet}$	80	121	218	225

Table XII. Amount of CPU time utilized in optimizing the geometry and calculating vibrational frequencies for D_{4h}-$M_2(O_2CH)_4^0$ at the B3LYP/SDD level of theory

	$Mo_2(O_2CH)_4$		$W_2(O_2CH)_4$	
	6-31G*	aug-cc-pVDZ	6-31G*	aug-cc-pVDZ
Geometry optimization	22.03 min	101.63 min	19.28 min	717.62 min
Frequency analysis	830.58 min	2920.88 min	810.75 min	4239.28 min

All calculations were performed on a SUN SunFire 6800 cluster with 900 MHz UltraSPARC III processors, each chip having a peak performance of 1.8 GFLOPS.

observable. For this reason, bar graphs are available in the Supporting Information to illustrate the signed-error of a particular basis set with respect to experimental observables. In general, all selected basis sets overestimated experimental observables at each level of theory. The only notable exception to this trend was in the case of the $\delta \rightarrow \delta^*$ transition energies. Discounting the 3-21G basis set, theory tended to overestimate the vertical transition energies in the neutral $M_2(O_2CH)_4$ complexes, while energies for the radical cations were underestimated.

Selecting the Appropriate Level of Theory: The Model Complexes D_{4h}-$[M_2(O_2CH)_4]^{0/+\bullet}$, D_{2h}-$[(HCO_2)_3M_2]_2(\mu\text{-}O_2CCO_2)]^{0/+\bullet}$, and D_{2h}-$[(HCO_2)_3M_2]_2(\mu\text{-}O_2CC_6F_6CO_2)]^{0/+\bullet}$ (M = Mo, W)

Compounds of the form $[(RCO_2)_3M_2]_2$-X-$[M_2(RCO_2)_3]_2$ (M = Mo, W; R = ^{t}Bu), where X is a dicarboxylate bridge such as oxalate or perfluoroterephthalate (both pictured in Fig. 2), constitute an active area of research in the laboratories of both Cotton and Chisholm [1, 26, 27, 36, 53–58, 61–74]. An ability to select the most suitable theoretical methodology for modeling bridged complexes is not a simple one. While the $[M_2(O_2CH)_4]^{0/+\bullet}$ model complexes are logical for testing basis sets, they may not be the most representative for selecting an XC functional. There are only 18 atoms in the model complexes $[M_2(O_2CH)_4]^{0/+\bullet}$, two of which are transition metals. D_{2h}-$[(HCO_2)_3M_2]_2(\mu\text{-}O_2CCO_2)]^{0/+\bullet}$ and D_{2h}-$[(HCO_2)_3M_2]_2(\mu\text{-}O_2CC_6F_6CO_2)]^{0/+\bullet}$, however, contain 34 and 44 atoms, respectively, with *four* transition metals per complex. Given the large number of electrons in the aforementioned systems, we investigated the effects of various XC functionals on the optimized geometries, vibrational frequencies, and excitation energies of D_{2h}-$[(HCO_2)_3M_2]_2(\mu\text{-}O_2CCO_2)]^{0/+\bullet}$ and D_{2h}-$[(HCO_2)_3M_2]_2(\mu\text{-}O_2CC_6F_6CO_2)]^{0/+\bullet}$. All complexes were evaluated at the B3LYP, B3P86, BPW91, and PW91PW91 levels of theory, utilizing a 6-31G* basis set on C, H, O, and F, and a SDD ECP on Mo and W. The results, coupled with those from the D_{4h}-$[M_2(O_2CH)_4]^{0/+\bullet}$ calculations, are compiled in Tables XIII–XV.

Reliable bond length data are only available for the D_{4h}-$[M_2(O_2C^tBu)_4]^{0/+\bullet}$ complexes (M = Mo, W), where single-crystal X-ray structures are available [49]. While X-ray powder diffraction studies have helped to elucidate certain structural features for D_{2h}-$[(^tBuCO_2)_3M_2]_2(\mu\text{-}O_2CCO_2)]$ and D_{2h}-$[(^tBuCO_2)_3M_2]_2(\mu\text{-}O_2CC_6F_6CO_2)]$ (M = Mo, W), they do not provide the quality of geometric data necessary for comparison [36, 54]. As shown in Table XIII, the hybrid B3P86 XC functional has the lowest overall MAE for D_{4h}-$[M_2(O_2C^tBu)_4]$ (M = Mo, W). The hybrid B3LYP XC functional slightly underperforms B3P86 by an average of 0.0119 Å, while both BPW91 and PW91PW91 underperform B3P86 by 0.0192 and 0.0174 Å, respectively.

Table XIII. Overall AEs and MAEs for M–M and M–O bond lengths (Å) in complexes of the form D_{4h}-$M_2(O_2CH)4^{0/+\bullet}$

Bond length	B3LYP AE	B3P86 AE	BPW91 AE	PW91PW91 AE
Mo_2	0.0317	0.0200	0.0533	0.0543
W_2	0.0245	0.0116	0.0397	0.0409
Mo–O	0.0106	0.0085	0.0054	0.0007
W–O	0.0307	0.0136	0.0262	0.0209
$Mo_2^{+\bullet}$	0.0147	0.0007	0.0325	0.0334
$W_2^{+\bullet}$	0.0228	0.0089	0.0352	0.0362
$Mo–O^{+\bullet}$	0.0122	0.0047	0.0134	0.0085
$W–O^{+\bullet}$	0.0326	0.0168	0.0331	0.0287
MAE neutral	0.0244	0.0134	0.0311	0.0292
$MAE^{+\bullet}$	0.0206	0.0078	0.0286	0.0267
MAE all	0.0225	0.0106	0.0298	0.0280

An assessment of which XC functional produces the most accurate vibrational frequencies was also undertaken. Raman assignments for the most intense active modes in D_{4h}-$[M_2(O_2C^tBu)_4]^{0/+\bullet}$ (M–M stretch), D_{2h}-$[(^tBuCO_2)_3M_2]_2(\mu\text{-}O_2CCO_2)]^{0/+\bullet}$ (M–M stretch, ν_1, ν_2, and ν_3 of oxalate) (Fig. 3), and D_{2h}-$[(^tBuCO_2)_3M_2]_2(\mu\text{-}O_2CC_6F_6CO_2)]^{0/+\bullet}$ (M–M stretch, δ_s CO_2 and ν_s CO_2, and ring stretching frequency of perfluoroterephthalate) (Fig. 2.4) (M = Mo, W) were compared to the calculated values for the model complexes. The results are compiled in Table XIV. Based on MAEs, the most accurate XC functionals were PW91PW91 and BPW91, respectively, followed very closely by B3LYP, which differed from PW91PW91 by ca. 4 cm^{-1}.

Various excitation energies were also calculated using TD-DFT. The $\delta \rightarrow \delta^*$ transitions for D_{4h}-$[M_2(O_2C^tBu)_4]^{0/+\bullet}$, as well as the D_{2h}-$[(HCO_2)_3M_2]_2(\mu\text{-}O_2CCO_2)]^{0/+\bullet}$ and D_{2h}-$[(HCO_2)_3M_2]_2(\mu\text{-}O_2CC_6F_6CO_2)]^{0/+\bullet}$ $[M_2]_2$ $\delta \rightarrow CO_2\pi^*$ and $[M_2]_2$ $\delta \rightarrow \delta$ IVCT transitions (Mo = Mo, W) were compared to experimental data where available.[4] The results, shown in Table XIV, are not very conclusive. While B3LYP has the lowest MAE of the four XC correlations tested, it is only 5 nm better than the least accurate. Individual AEs yield no special insight either. For example, AEs for W complexes tend to be higher than for Mo at the B3lYP and B3P86 levels of theory; from the AEs for the D_{4h}-$[W_2(O_2C^tBu)_4]^{+\bullet}$ $\delta \rightarrow \delta^*$ and D_{2h}-$[(HCO_2)_3W_2]_2(\mu\text{-}O_2CC_6F_6CO_2)]^{+\bullet}$ $\delta \rightarrow \delta$ IVCT transition energies, though, it is easy to see that this does not hold true. A meaningful

[4]The IVCT transitions only apply to the radical cations.

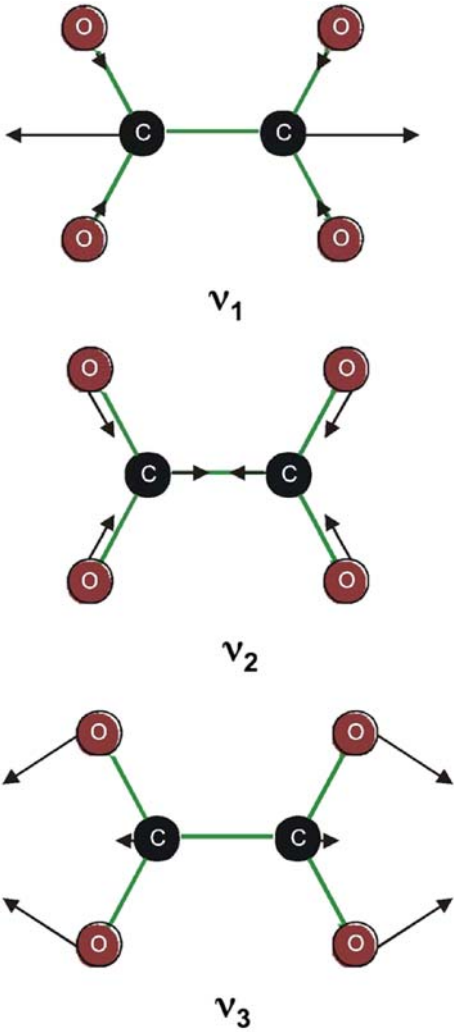

Fig. 3. Some normal mode vibrations of the oxalate dianion.

observation *can* be made if the AEs of the M_4 $\delta \rightarrow \delta$ IVCT results are treated as outliers.

Since AEs for the M_4 $\delta \rightarrow \delta$ IVCT transition are off by one—and in many cases two—orders of magnitude from other AEs, and since they have been poorly modeled in the past[36,54], they were removed from treatment of the TD-DFT radical cation data. This adjustment shows both BPW91 and

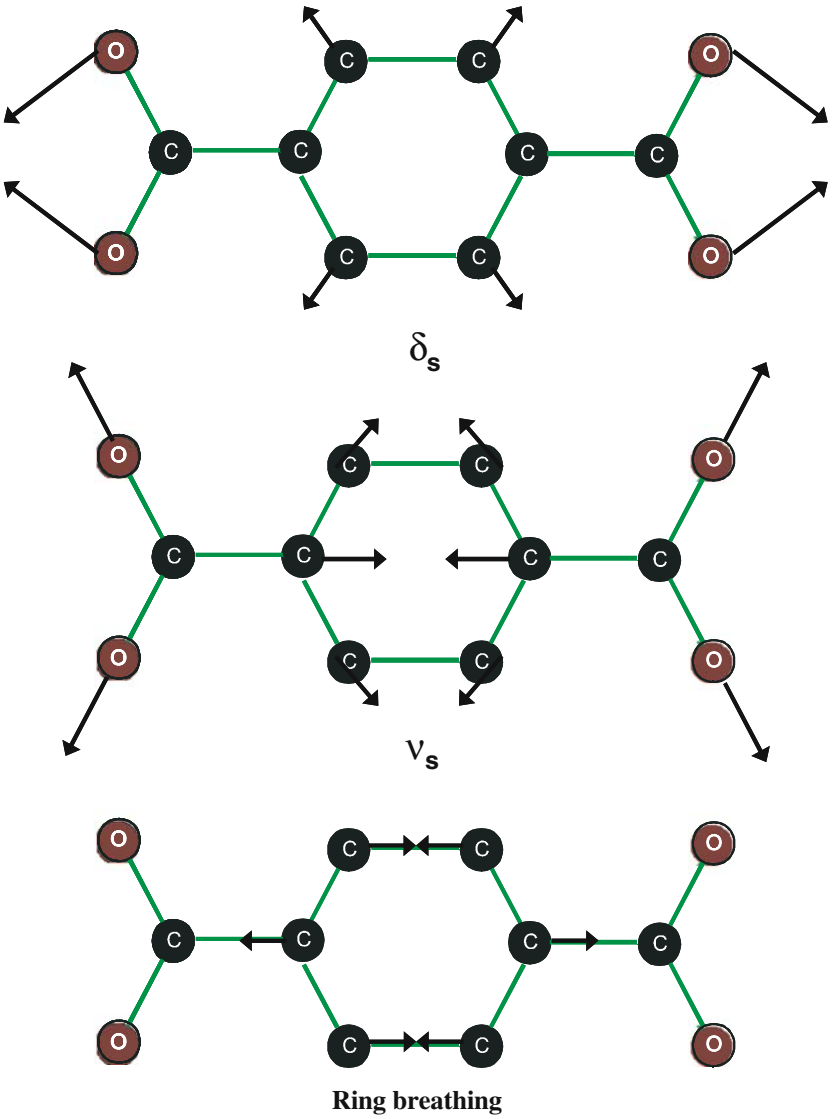

Fig. 4. Some normal mode vibrations of the perfluoroterepthalate dianion.

PW91PW91 to be more accurate than B3LYP and B3P86 by ca. 30 nm (Table XV), with the overall MAEs reflecting this improvement. As previously mentioned, though, MAEs alone do not paint a complete picture of the quality of results. The magnitude of the errors also needs to be

Table XIV. Overall AEs and MAEs for stretching vibrational frequencies (cm^{-1}) in complexes of the form D_{4h}-$M_2(O_2CH)_4^{0/+\bullet}$ (F), D_{2h}-$[(HCO_2)_3M_2]_2(\mu\text{-}O_2CCO_2)]^{0/+\bullet}$ (O), and D_{2h}-$[(HCO_2)_3M_2]_2(\mu\text{-}O_2CC_6F_6CO_2)]^{0/+\bullet}$ (P)

Vibrational modes	B3LYP AE	B3P86 AE	BPW91 AE	PW91PW91 AE
Mo_2 (F)	60.93	72.13	42.65	42.90
Mo_4 (O)	9.06	1.99	16.42	12.24
ν_1 (O)	35.07	45.82	0.47	2.69
ν_2 (O)	38.18	63.56	31.48	22.49
ν_3 (O)	18.57	26.17	3.35	7.12
Mo_4 (P)	71.07	79.07	29.32	28.49
(P) CO_2 δ_s	8.78	16.48	4.41	0.49
(P) CO_2 ν_s	315.56	301.72	349.18	343.86
(P) ring st.	29.00	49.22	29.83	22.29
W_2 (F)	20.48	29.22	8.68	7.91
W_4 (O)	29.84	38.86	18.04	17.07
ν_1 (O)	18.60	30.08	19.68	17.36
ν_2 (O)	68.21	96.51	33.18	44.62
ν_3 (O)	16.54	24.74	4.77	9.10
W_4 (P)	27.07	35.49	15.33	14.38
(P) CO_2 δ_s	11.11	19.79	1.33	5.63
(P) CO_2 ν_s	184.10	169.89	219.22	214.41
(P) ring st.	6.62	13.42	60.28	52.88
Mo_4 $(F)^{+\bullet}$	42.90	55.77	28.83	30.50
Mo_4 $(O)^{+\bullet}$	51.01	61.71	39.51	35.72
ν_1 $(O)^{+\bullet}$	22.06	32.49	13.47	10.32
ν_2 $(O)^{+\bullet}$	47.71	98.31	28.52	40.08
ν_3 $(O)^{+\bullet}$	3.25	11.83	20.65	9.51
W_4 $(O)^{+\bullet}$	25.51	33.89	16.03	12.92
ν_1 $(O)^{+\bullet}$	9.05	21.91	14.68	16.38
ν_2 $(O)^{+\bullet}$	15.52	45.59	27.82	7.15
ν_3 $(O)^{+\bullet}$	4.96	3.89	34.23	21.26
MAE neutral	53.82	61.90	49.31	48.11
$MAE^{+\bullet}$	24.66	40.60	24.86	20.43
MAE all	39.24	51.25	37.09	34.27

examined in order to make a judicious decision as to which methodology is more appropriate. As shown in the Supporting Information, however, there is no discernable trend in any of the calculated parameters, across any of the methods. This leaves us with an interesting question—*is* there a single ''best method'' for electronic structure calculations on M_2 multiply bonded complexes?

The problem of selecting XC functional has almost become a problem of splitting hairs. It is clear the B3P86 XC functional should be avoided.

Table XV. Overall AEs and MAEs for vertical excitation energies (nm) in complexes of the form D_{4h}-$M_2(O_2CH)_4^{0/+\bullet}$ (F), D_{2h}-$[(HCO_2)_3M_2]_2(\mu\text{-}O_2CCC_2)]^{0/+\bullet}$ (O), and D_{2h}-$[(HCO_2)_3M_2]_2(\mu\text{-}O_2CC_6F_6CO_2)]^{0/+\bullet}$ (P)

Excitation energy	B3LYP AE	B3P86 AE	BPW91 AE	PW91PW91 AE
$Mo_2\ \delta \rightarrow\ \delta^*$ (F)	72	45	9	6
$Mo_4\ \delta \rightarrow\ CO_2\pi^*$ (O)	11	15	63	63
$Mo_4\ \delta \rightarrow\ CO_2\pi^*$ (P)	46	43	156	151
$W_4\ \delta \rightarrow\ CO_2\pi^*$ (O)	175	184	133	134
$W_4\ \delta \rightarrow\ CO_2\pi^*$ (P)	208	217	145	147
$Mo_2\ \delta \rightarrow\ \delta^*\ (F)^{+\bullet}$	140	53	132	140
$Mo_4\ \delta \rightarrow\ CO_2\pi^*\ (O)^{+\bullet}$	180	201	95	97
$Mo_4\ \delta \rightarrow\ \delta\ (O)^{+\bullet}$	1079	1124	1181	1193
$W_2\ \delta \rightarrow\ \delta^*\ (F)^{+\bullet}$	71	117	216	222
$W_4\ \delta \rightarrow\ CO_2\pi^*\ (O)^{+\bullet}$	116	125	60	52
$W_4\ \delta \rightarrow\ \delta\ (O)^{+\bullet}$	520	545	478	468
$W_4\ \delta \rightarrow\ CO_2\pi^*\ (P)^{+\bullet}$	249	257	149	151
$W_4\ \delta \rightarrow\ \delta\ (P)^{+\bullet}$	1831	1857	1926	1937
MAE neutral	102	101	101	100
$MAE^{+\bullet}$	523	535	530	533
MAE all	313	318	316	317

Even though the B3P86 method generates the lowest bond length MAE, it also produces the least accurate vibrational frequencies (by ca. 17 cm^{-1} relative to the lowest MAE) and excitation wavelengths (by ca. 16 nm if the IVCT transitions are neglected). The choice, then, is between B3LYP, BPW91, and PW91PW91. Of the three, B3LYP has the lowest bond length MAE, but a vibrational frequency MAE ca. 5 cm^{-1} less accurate than PW91PW91. PW91PW91, however, is only 0.0055 Å less accurate than B3LYP, and it has the lowest vibrational frequency MAE of all the methods examined. PW91PW91 also outperforms B3LYP by 25 nm when describing the radical cation excitation energies. BPW91, however, has the highest bond length and vibrational frequency MAEs, being 0.0018 Å and 2.82 cm^{-1} less accurate, respectively, than PW91PW91.

With the aforementioned information, the question posed earlier, ''*is* there a single ''best method'' for electronic structure calculations on M_2 multiply bonded complexes?'' should perhaps be recast as, ''is the use of the B3LYP XC functional *justified*''? The answer to this question is yes, but there is a caveat. While PW91PW91 performs slightly better than B3LYP *for the parameters considered in this study*, the difference in MAEs between the two are still quite small. There is also a matter of precedence; the test set of molecules for B3LYP is more established than for PW91PW91. A SciFinder

Scholar search for B3LYP solicited over 16,000 journal articles, while the same search only found ca. 270 articles concerning PW91PW91. The ultimate choice of XC functional for M_2 bonded systems, then, is more a matter of taste than a matter of relying on the statistics of small numbers. As more experimental data for M_2 bridged complexes becomes available, this attitude should be re-evaluated accordingly.

CONCLUSIONS

Electronic structure calculations at a variety of DFT levels have been carried out in order to evaluate their efficacy and cost-effectiveness. Various basis sets and XC functionals were used to calculate geometries, stretching vibrational frequencies, and vertical electronic excitation energies for model complexes of the form D_{4h}-$[M_2(O_2CH)_4]^{0/+\bullet}$, D_{2h}-$[(HCO_2)_3M_2]_2(\mu$-$O_2CCO_2)]^{0/+}$, and D_{2h}-$[(HCO_2)_3M_2]_2(\mu$-$O_2CC_6F_6CO_2)]^{0/+\bullet}$ (M = Mo, W). The most effective basis sets were found to be the SDD ECP on Mo and W, with a 6-31G* Pople style basis set on all non-metal atoms. Both B3LYP and PW91PW91 gave the most accurate results overall, with PW91PW91 giving slightly better vibrational frequencies and excitation wavelengths. PW91PW91 does perform better (when the IVCT results are omitted) for calculating the excitation wavelengths of the radical cations.

Future work in this area should entail further benchmarking as more experimental data become available. It would also be prudent to benchmark the formamidinate systems of Cotton and coworkers, to ascertain whether or not there are major differences relative to our carboxylate systems. Since our complexes are known to be solvatochromic [75], it would also be instructional to investigate solvent models in the calculation of vibrational frequencies and excitation energies.

ACKNOWLEDGMENTS

The authors gratefully acknowledge the National Science Foundation for funding, and the Ohio Supercomputing Center for its generous allocation of computational resources. JSD gratefully acknowledges Professor Bruce Bursten and Dr. Jason Sonnenberg for fruitful discussions.

REFERENCES

1. F. A. Cotton and R. A. Walton, *Multiple Bonds Between Metal Atoms* (Clarendon Press, Oxford, 1993).
2. W. Klotzbuecher, G. A. Ozin, J. G. Norman Jr., and H. J. Kolari (1977). *Inorg. Chem.* **16**, 2871.

3. J. G. Norman Jr., H. J. Kolari, H. B. Gray, and W. C. Trogler (1977). *Inorg. Chem.* **16**, 987.
4. J. G. Norman Jr. and H. J. Kolari (1975). *J. Chem. Soc., Chem. Commun.* 649.
5. F. A. Cotton and C. B. Harris (1965). *Inorg. Chem.* **4**, 330.
6. L. Noodleman and J. G. Norman Jr. (1979). *J. Chem. Phys.* **11**, 4903.
7. J. G. Norman Jr., G. E. Renzoni, and D. A. Case (1979). *J. Am. Chem. Soc.* **101**, 5256.
8. T. Ziegler (1985). *J. Am. Chem. Soc.* **107**, 4453.
9. M. D. Braydich, B. E. Bursten, M. H. Chisholm, and D. L. Clark (1985). *J. Am. Chem. Soc.* **107**, 4459.
10. F. A. Cotton, V. M. Miskowski, and B. Zhong (1989). *J. Am. Chem. Soc.* **111**, 6177.
11. D. J. Santure, J. C. Huffman, and A. P. Sattelberger (1985). *Inorg. Chem.* **24**, 371.
12. M. D. Hopkins, H. B. Gray, and V. M. Miskowski (1987). *Polyhedron* **6**, 705.
13. B. E. Bursten and T. W. Clayton Jr. (1994). *J. Cluster Sci.* **5**, 157.
14. V. M. Miskowski, M. D. Hopkins, J. R. Winkler, and H. B. Gray, *in* E. I. Solomon and A. B. P. Lever (eds.), *Inorganic Electronic Structure and Spectroscopy* (John Wiley and Sons, Inc., 1999), pp. 343–402.
15. F. A. Cotton and D. G. Nocera (2000). *Acc. Chem. Res.* **33**, 483.
16. M. B. Hall (1987). *Polyhedron* **6**, 679.
17. J. C. Slater (1965). *J. Chem. Phys.* **43**, S228.
18. K. H. Johnson (1966). *J. Chem. Phys.* **45**, 3085.
19. F. A. Cotton and X. Feng (1997). *J. Am. Chem. Soc.* **119**, 7514.
20. F. A. Cotton and X. Feng (1998). *J. Am. Chem. Soc.* **120**, 3387.
21. T. H. Dunning Jr. and P. J. Hay, *in* H. F. Schaefer, (ed.), *Modern Theoretical Chemistry* (Los Alamos Sci. Lab., University of California, Los Alamos, NM, USA, 1977), pp 1–27.
22. P. J. Hay and W. R. Wadt (1985). *J. Chem. Phys.* **82**, 270.
23. P. J. Hay and W. R. Wadt (1985). *J. Chem. Phys.* **82**, 299.
24. W. R. Wadt and P. J. Hay (1985). *J. Chem. Phys.* **82**, 284.
25. F. A. Cotton, G. Gu, C. A. Murillo, and D. J. Timmons (1999). *J. Chem. Soc., Dalton Trans.* **21**, 3741.
26. F. A. Cotton, J. P. Donahue, C. A. Murillo, and L. M. Perez (2003). *J. Am. Chem. Soc.* **125**, 5486.
27. F. A. Cotton (2003). *J. Am. Chem. Soc.* **125**, 8900.
28. F. A. Cotton, C. Y. Liu, C. A. Murillo, D. Villagran, and X. Wang (2004). *J. Am. Chem. Soc.* **126**, 14822.
29. A. D. Becke (1993). *J. Chem. Phys.* **98**, 5648.
30. C. Lee, W. Yang, and R. G. Parr (1988). *Phys. Rev. B: Condens. Matter.* **37**, 785.
31. A. D. Becke (1988). *Phys. Rev. A: At. Mol. Opt. Phys.* **38**, 3098.
32. W. Koch and M. C. Holthausen, *A Chemist's Guide to Density Functional Theory* (Wiley-VCH, Chichester, 2000).
33. W. J. Hehre, L. Radom, P. v. R. Schleyer, and J. A. Pople, *Ab initio Molecular Orbital Theory* (John Wiley & Sons, New York, 1986).
34. D. Andrae, U. Hauessermann, M. Dolg, and H. Preuss (1990). *Theor. Chim. Acta* **77**, 123.
35. M. J. Frisch, G. W. Trucks, H. B. Schlegel, G. E. Scuseria, M. A. Robb, J. R. Cheeseman, J. A. Montgomery Jr., T. Vreven, K. N. Kudin, J. C. Burant, J. M. Millam, S. S. Iyengar, J. Tomasi, V. Barone, B. Mennucci, M. Cossi, G. Scalmani, N. Rega, G. A. Petersson, H. Nakatsuji, M. Hada, M. Ehara, K. Toyota, R. Fukuda, J. Hasegawa, M. Ishida, T. Nakajima, Y. Honda, O. Kitao, H. Nakai, M. Klene, X. Li, J. E. Knox, H. P. Hratchian, J. B. Cross, C. Adamo, J. Jaramillo, R. Gomperts, R. E. Stratmann, O. Yazyev, A. J. Austin, R. Cammi, C. Pomelli, J. W. Ochterski, P. Y. Ayala, K. Morokuma, G. A. Voth, P. Salvador, J. J. Dannenberg, V. G. Zakrzewski, S. Dapprich, A. D. Daniels, M. C. Strain, O. Farkas, D. K. Malick, A. D. Rabuck, K. Raghavachari, J. B. Foresman, J. V. Ortiz,

Q. Cui, A. G. Baboul, S. Clifford, J. Cioslowski, B. B. Stefanov, G. Liu, A. Liashenko, P. Piskorz, I. Komaromi, R. L. Martin, D. J. Fox, T. Keith, M. A. Al-Laham, C. Y. Peng, A. Nanayakkara, M. Challacombe, P. M. W. Gill, B. Johnson, W. Chen, M. W. Wong, C. Gonzalez, and J. A. Pople, *Gaussian 03*, Revision B.01 and C.02 (Gaussian, Inc., Pittsburgh, PA, 2003).
36. B. E. Bursten, M. H. Chisholm, R. J. H. Clark, S. Firth, C. M. Hadad, P. J. Wilson, P. M. Woodward, and J. M. Zaleski (2002). *J. Am. Chem. Soc.* **124**, 12244.
37. J. P. Perdew (1986). *Phys. Rev. B: Condens. Matter*. **33**, 8822.
38. K. Burke, J. P. Perdew, and Y. Wang, in *Derivation of a Generalized Gradient Approximation: The PW91 Density Functional, Electronic Density Functional Theory: Recent Progress and New Directions* [Proceedings of the International Workshop on Electronic Density Functional Theory: Recent Progress and New Directions] (Nathan, Australia, July 14–19, 1996, 1998; 1998), pp. 81–111.
39. J. P. Perdew, K. Burke, and Y. Wang (1996). *Phys. Rev. B: Condens. Matter*. **54**, 16533.
40. J. P. Perdew, J. A. Chevary, S. H. Vosko, K. A. Jackson, M. R. Pederson, D. J. Singh, and C. Fiolhais (1993). *Rev. B: Condens. Matter* **48**, 4978.
41. J. P. Perdew, J. A. Chevary, S. H. Vosko, K. A. Jackson, M. R. Pederson, D. J. Singh, and C. Fiolhais (1992). *Phys. Rev. B: Condens. Matter* **46**, 6671.
42. J. P. Perdew, *in* P. Ziesche and H. Eschrig (eds.), *Electronic Structure of Solids* (Akademie Verlag, Berlin, 1991), p. 11.
43. J. P. Perdew, K. Burke, and M. Ernzerhof (1997). *Phys. Rev. Lett*. **78**, 1396.
44. J. P. Perdew, K. Burke, and M. Ernzerhof (1996). *Phys. Rev. Lett*. **77**, 3865.
45. J. P. Perdew and Y. Wang (1992). *Phys. Rev. B: Condens. Matter* **45**, 13244.
46. R. Bauernschmitt and R. Ahlrichs (1996). *Chem. Phys. Lett*. **256**, 454.
47. M. E. Casida, C. Jamorski, K. C. Casida, and D. R. Salahub (1998). *J. Chem. Phys*. **108**, 4439.
48. R. E. Stratmann, G. E. Scuseria, and M. J. Frisch (1998). *J. Chem. Phys*. **109**, 8218.
49. M. H. Chisholm, J. S. D'Acchioli, B. D. Pate, N. J. Patmore, N. S. Dalal, and D. J. Zipse (2005). *Inorg. Chem*. **44**, 1061.
50. F. Jensen, *Introduction to Computational Chemistry* (Wiley, New York, 1999).
51. N. Kaltsoyannis (1997). *J. Chem. Soc., Dalton Trans*. 1–11.
52. F. Furche and J. P. Perdew (2006). *J. Chem. Phys*. 124.
53. M. J. Byrnes and M. H. Chisholm (2002). *Chem. Commun*. 2040.
54. B. E. Bursten, M. H. Chisholm, R. J. H. Clark, S. Firth, C. M. Hadad, A. M. MacIntosh, P. J. Wilson, P. M. Woodward, and J. M. Zaleski (2002). *J. Am. Chem. Soc*. **124**, 3050.
55. F. A. Cotton, C. Y. Liu, C. A. Murillo, D. Villagran, and X. Wang (2003). *J. Am. Chem. Soc*. **125**, 13564.
56. M. H. Chisholm (2003). *Dalton Trans*. 3821.
57. M. J. Byrnes, M. H. Chisholm, R. J. H. Clark, J. C. Gallucci, C. M. Hadad, and N. J. Patmore (2004). *Inorg. Chem*. **43**, 6334.
58. M. H. Chisholm, R. J. H. Clark, C. M. Hadad, and N. J. Patmore (2004). *Chem. Commun*. 80.
59. B. E. Bursten, M. H. Chisholm, and J. S. D'Acchioli (2005). *Inorg. Chem*. **44**, 5571.
60. E. J. Baerends, J. A. Autschbach, A. Bérces, C. Bo, P. M. Boerrigter, L. Cavallo, D. P. Chong, L. Deng, R. M. Dickson, D. E. Ellis, L. Fan, T. H. Fischer, C. F. Fonseca Guerra, S. J. A. van Gisbergen, J. A. Groeneveld, O. V. Gritsenko, M. Grüning, F. E. Harris, P. van den Hoek, H. Jacobsen, G. van Kessel, F. Kootstra, E. van Lenthe, V. P. Osinga, S. Patchkovskii, P. H. T. Philipsen, D. Post, C. C. Pye, W. Ravenek, P. Ros, P. R. T. Schipper, G. Schreckenbach, J. G. Snijders, M. Sola, M. Swart, D. Swerhone, G. te Velde, P. Vernooijs, L. Versluis, O. Visser, E. van Wezenbeek, G. Wiesenekker,

S. K. Wolff, T. K. Woo, and T. Ziegler *ADF*, 2002.03; www.scm.com (Amsterdam, The Netherlands, 2003).
61. R. H. Cayton, M. H. Chisholm, J. C. Huffman, and E. B. Lobkovsky (1991). *J. Am. Chem. Soc.* **113**, 8709.
62. F. A. Cotton, Y. Kim, and T. Ren (1992). *Inorg. Chem.* **31**, 2723.
63. F. A. Cotton, L. M. Daniels, C. Lin, C. A. Murillo, and S.-Y. Yu (2001). *J. Chem. Soc. Dalton Trans.* 502.
64. F. A. Cotton, C. Lin, and C. A. Murillo (2001). *Inorg. Chem.* **40**, 478.
65. F. A. Cotton, C. Lin, and C. A. Murillo (2001). *Acc. Chem. Res.* **34**, 759.
66. F. A. Cotton, C. Lin, and C. A. Murillo (2001). *Inorg. Chem.* **40**, 6413.
67. J. K. Bera, P. Angaridis, F. A. Cotton, M. A. Petrukhina, P. E. Fanwick, and R. A. Walton (2001). *J. Am. Chem. Soc.* **123**, 1515.
68. B. E. Bursten, M. H. Chisholm, C. M. Hadad, J. Li, and P. J. Wilson (2001). *Isr. J. Chem.* **41**, 187.
69. F. A. Cotton, C. Lin, and C. A. Murillo (2002). *Proc. Natl. Acad. Sci. U.S.A.* **99**, 4810.
70. M. H. Chisholm, B. D. Pate, P. J. Wilson, and J. M. Zaleski (2002). *Chem. Commun.* 1084.
71. M. H. Chisholm (2002). *J. Organomet. Chem.* **641**, 15.
72. F. A. Cotton (2003). *J. Am. Chem. Soc.* **125**, 5436.
73. P. Angaridis, J. F. Berry, F. A. Cotton, C. A. Murillo, and X. Wang (2003). *J. Am. Chem. Soc.* **125**, 10327.
74. F. A. Cotton, Y. Liu Chun, A. Murillo Carlos, D. Villagran, and X. Wang (2004). *J. Am. Chem. Soc.* **126**, 14822.
75. M. H. Chisholm and N. J. Patmore (2004). *Inorg. Chim. Acta* **357**, 3877.